Journal of Power Sources 185 (2008) 445–450

Contents lists available at ScienceDirect

Journal of Power Sources

journal homepage: www.elsevier.com/locate/jpowsour

A self-regulating hydrogen generator for micro fuel cells

Saeed Moghaddam[a,*], Eakkachai Pengwang[a], Richard I. Masel[b], Mark A. Shannon[a]

[a] Mechanical Science and Engineering, University of Illinois at Urbana-Champaign, 1206 West Green Street, Urbana, IL 61801, United States
[b] Chemical and Biomolecular Engineering, University of Illinois at Urbana-Champaign, 213 Roger Adams Lab, 600 S. Mathews, Urbana, IL 61801, United States

ARTICLE INFO

Article history:
Received 29 May 2008
Received in revised form 16 June 2008
Accepted 17 June 2008
Available online 3 July 2008

Keywords:
Fuel cell
Hydrogen generation
Passive control
Metal hydride
Microvalve
Power source for portable applications

ABSTRACT

The ever-increasing power demands and miniaturization of portable electronics, micro-sensors and actuators, and emerging technologies such as cognitive arthropods have created a significant interest in development of micro fuel cells. One of the major challenges in development of hydrogen micro fuel cells is the fabrication and integration of auxiliary systems for generating, regulating, and delivering hydrogen gas to the membrane electrode assembly (MEA). In this paper, we report the development of a hydrogen gas generator with a micro-scale control system that does not consume any power. The hydrogen generator consists of a hydride reactor and a water reservoir, with a regulating valve separating them. The regulating valve consists of a port from the water reservoir and a movable membrane with via holes that permit water to flow from the reservoir to the hydride reactor. Water flows towards the hydride reactor, but stops within the membrane via holes due to capillary forces. Water vapor then diffuses from the via holes into the hydride reactor resulting in generation of hydrogen gas. When the rate of hydrogen consumed by the MEA is lower than the generation rate, gas pressure builds up inside the hydride reactor, deflecting the membrane, closing the water regulator valve, until the pressure drops, whereby the valve reopens. We have integrated the self-regulating micro hydrogen generator to a MEA and successfully conducted fuel cell tests under varying load conditions.

Published by Elsevier B.V.

1. Introduction

The increasing demand for high energy density power sources driven by advancements in portable electronics and MEMS devices has generated significant interest in development of micro fuel cells and batteries [1,2]. In terms of energy density, metal hydrides (e.g. $NaBH_4$), methanol, and most hydrocarbon fuels have an energy density up to an order of magnitude higher than the competitive battery technologies. Micro fuel cells, however, can potentially outperform the batteries only if their fuel to device volume ratio can be maximized and the power consumption of their auxiliary systems to regulate fuel delivery and power output is significantly reduced. While fabrication of small-scale membrane electrode assembly (MEA) is widely reported in literature [3–8], shrinking the size of the auxiliary systems (pump, valves, sensors, distribution components, and power and control electronics for these components) has remained a challenge. While this might be somewhat feasible in centimeter-scale fuel cells, fitting all the auxiliary components within a few cubic millimeters volume is quite a challenge. Developing a new means of fuel delivery and control that can be scaled downed and consume little to no power opens an opportunity for fabricating millimeter-scale fuel cells and realizing new devices that are tied to the existence of such power sources.

Despite the advancements in fuel cell components and fabrication processing, there has been very little progress made on micro fuel cell system integration. Integrated micro fuel cell architectures suggested in literature (e.g. in [9–12]) are scaled-downed versions of large-scale systems with numerous auxiliary components. These components can be much larger than the membrane electrode assembly, greatly reducing the overall device energy density. In addition, they consume power, which reduces available output power from the micro fuel cell for a further reduction of the device energy density. Additionally, auxiliary components normally require numerous microfabrication steps and have integration difficulties that can result in higher production costs and added complexity of micro fuel cells operation.

Examples of fuel delivery and control systems can be found in [13–18]. Sarata et al. [13] proposed a pressure-based control system for a hydrogen generator comprising of a hydride reactor and water for hydrolysis. The hydrogen generation rate is controlled by monitoring the reactor pressure and then stopping the pumping of water to the hydride chamber when the hydride chamber pressure increases above a reference value. The pressure sensor, pump, valve, and electronics to conduct this control operation occupy significant space, which directly translate to lower energy density and

* Corresponding author. Tel.: +1 217 244 5136; fax: +1 217 244 6534.
E-mail addresses: saeedmog@uiuc.edu (S. Moghaddam), epengwa2@uiuc.edu (E. Pengwang), r-masel@uiuc.edu (R.I. Masel), mshannon@uiuc.edu (M.A. Shannon).

0378-7753/$ – see front matter. Published by Elsevier B.V.
doi:10.1016/j.jpowsour.2008.06.060

high cost for micro fuel cells. In another approach [18], the pressure increase in a macro-scale hydride chamber was used to automatically push the water out of a conduit that connected the water reservoir to the hydride reactor. This results in an increase in the diffusion length between the water front and the hydride and consequently slows down the hydrogen generation rate. This passive approach may be more suitable for miniaturization (e.g. fabrication of a microchannel between the water and hydride reservoirs and so on). But, unfortunately, since water diffusion and thereby hydrogen generation is not completely stopped, pressure continues to rise such that failure can occur. Furthermore, the movements of the water front inside the microchannel (i.e. dynamics of the advancing and receding contact lines) and the pressure of the excess hydrogen inside the device that pushes against the water front can be complicated to predict and control.

In this manuscript, we present the development of a micro hydrogen generator with a self-regulating control mechanism. The control scheme enables the hydrogen generator to automatically stop generating hydrogen when it is not consumed by the micro fuel cell. The volume of the control mechanism is less than 50 nL (approximately 0.5% of the device volume) and requires no energy input. This technology has enabled fabrication of the first fully integrated millimeter-scale fuel cell that operates much like a battery. This technology can also be implemented in centimeter-scale micro fuel cells to enhance their energy density and reliability and reduce their complexity and cost. Details of the control mechanism and development of a self-regulating micro hydrogen generator and its integration with a MEA are discussed in this manuscript.

2. Operation principle

The no-power, self-regulating hydrogen generator consists of a hydride reactor and a water reservoir, with a regulating valve separating them, as shown in Fig. 1. The regulating valve consists of a port and a membrane with via holes in it. Water flows through the port towards the hydride chamber, but stops within the membrane via holes due to capillary forces. Water vapor then diffuses into the hydride chamber resulting in hydrogen generation (metal hydrides such as LiH, $LiAlH_4$, and CaH_2 react with water vapor to produce H_2 [19]). When the rate of hydrogen consumption by the fuel cell is lower than generation rate, gas pressure builds up inside the hydride reactor and deflects the membrane towards the water port, blocking the port and ceasing the water flow to the hydride after the water evaporates. This regulation action, however, assumes that the membrane deflects under a smaller pressure than needed to break into the liquid meniscus formed inside the membrane via holes. Under such conditions, complete isolation of the hydride reactor from the water reservoir can occur. When hydrogen consumption by the fuel cell is faster than the generation rate, the reverse happens, opening the membrane to allow water to diffuse into the hydride reactor, increasing the hydrogen generation. Essentially, the control mechanism is a passive valve that automatically regulates hydrogen production based on the hydride reactor pressure. Details of the valve operation and testing are discussed in the following sections.

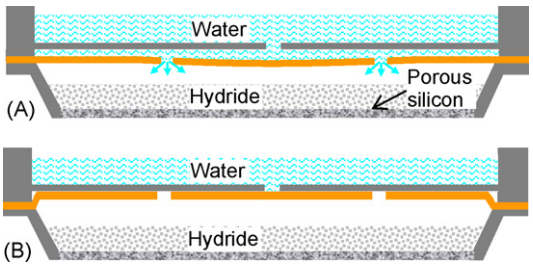

Fig. 1. Schematic cross-section of the self-regulating hydrogen generator and its principle of operation. (A) Membrane in release mode: water exits the reservoir and diffuses into the hydride reactor through the membrane holes. (B) Membrane in closed mode: small pressure buildup in the hydride reactor, when hydrogen is not used, bends the membrane and closes off the water port.

3. Valve fabrication and testing

3.1. Valve and water reservoir assembly

The membrane separating the water reservoir and the hydride reactor was made of polyimide (PI) through spinning and curing PI 5878G (from HD Microsystems) on a 100 mm diameter 500 μm thick glass wafer. The final thickness of the PI layer was 5 μm. A circular 1.3 mm diameter area at the center of the membrane was sputter coated with a 0.2 μm thick Cr/Au layer to prevent water diffusion through the membrane when it is closed. A circularly distributed array of 30 μm diameter holes was etched through the Cr/Au (wet etched) and PI (reactive ion etched) layers close to the perimeter of the Cr/Au coated area. Fig. 2 shows the front view of the membrane. The membrane was then transfer-bonded (process is described in [20]) to the bottom of the water reservoir fabricated from ⟨1 0 0⟩ *p*-doped silicon through deep reactive ion etching (DRIE) process (cf. Fig. 3). Note that the 3 μm deep recess seen in the bottom view of the reservoir is the separating gap between the PI membrane and the bottom of the water reservoir, as depicted in the schematic of Fig. 1.

3.2. Membrane bulge test

A test piece was fabricated to determine the membrane deflection with pressure. The test piece was a silicon die (10 mm × 10 mm) with 2.4 mm × 2.4 mm opening at its middle, over which the PI membrane was bonded. The PI membrane was similar to that of the device in every aspect (i.e. size and microfabrication process) except that it did not have the 30 μm holes. A bulge test setup was used to measure the membrane deflection at different pressures (cf. Fig. 4). The test piece was installed on the pressure chamber of the setup, as depicted in Fig. 4. The chamber pressure was increased using a piezoelectric actuator. As the results in Fig. 5 show, an applied pressure of approximately 150 Pa is sufficient to deform the

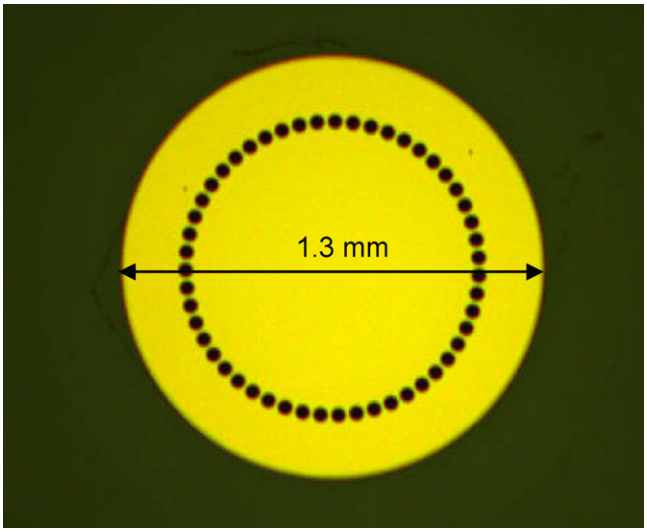

Fig. 2. Top view of the center of the polyimide membrane coated with Cr/Au to prevent water diffusion through the membrane. The holes are 30 μm in diameter.

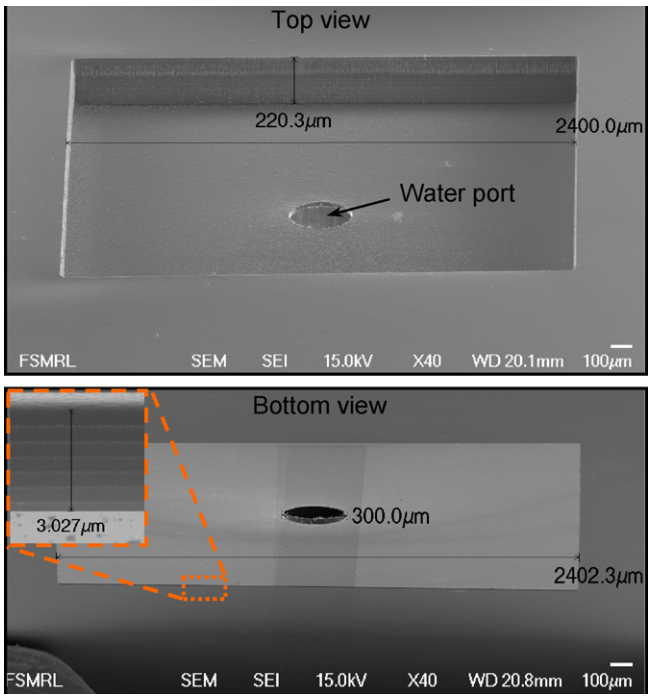

Fig. 3. Top and bottom views of the water reservoir. The inset figure in the bottom view shows a 3 μm deep recess that separates the reservoir from the PI membrane. Thickness of the reservoir bottom wall is 20 μm.

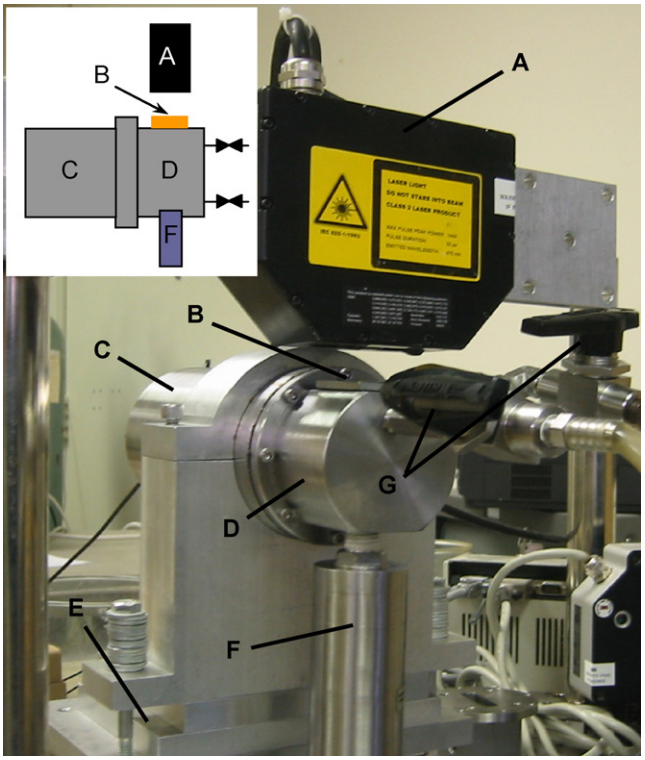

Fig. 4. Bulge test setup. Main system components: (A) laser sensor model 812330-SLS 700/15 from LMI Selcom, Inc., (B) a jig for holding the test article, (C) piezoelectric actuator model P-239.60 HVPZT from Physik Instrumente GmbH and Co. KG, (D) water chamber, (E) micro positioning stage, (F) pressure transducer model PX 309-001GV S5V from OMEGA Co., and (G) water inlet and outlet valves. The test article is attached to the jig (B). The micro positioning stage is used to adjust the sample right below the optical sensor. Next, the water chamber (D) is filled with water using the inlet and outlet valves (G). The water level reaches the top of the water chamber, but does not come into contact with the membrane.

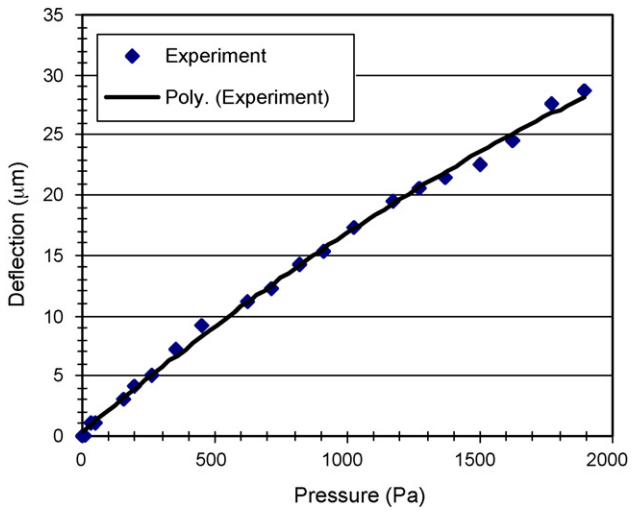

Fig. 5. Membrane deflection versus applied pressure.

membrane 3 μm. This pressure is significantly less than the typical water capillary pressure in the micro-scale via holes. For example, capillary pressure in a 30 μm hole with a surface to liquid contact angle of $\theta = 50$ degrees is approximately 6 kPa ($=2\sigma\cos\theta/r$). This suggests that the membrane will deflect and seal the water port before hydrogen can break the capillary meniscus formed inside the membrane holes.

3.3. Valve performance test

An experimental setup was fabricated to test the valve performance. The setup determines the open and close states of the valve as well as the water vapor released rate through the holes when the valve is open. Fig. 6 shows a schematic of the setup. The setup consists of two main chambers C-1 and C-2. Pressure inside each chamber is adjusted by changing the liquid (Fomblin oil) level in

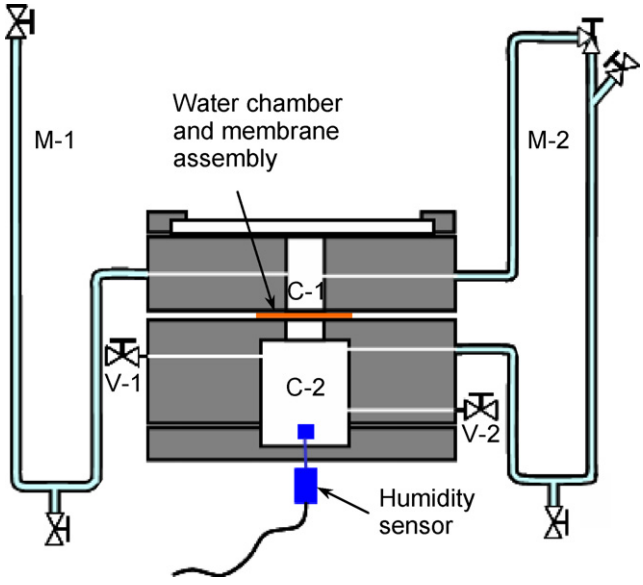

Fig. 6. Schematic of the test setup for measuring the valve performance. Schematic shows the water chamber and membrane assembly held between the top (C-1) and bottom (C-2) chambers of the setup. Two valves (V-1 and V-2) on the C-2 chamber are used for purging it with dry nitrogen. Two manometers (M-1 and M-2) are used to measure and adjust the pressure in C-1 and C-2 chambers.

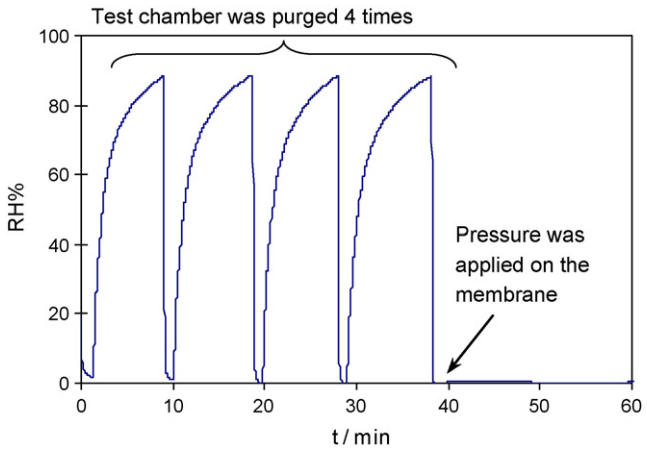

Fig. 7. Performance of the valve tested in the test setup shown in Fig. 6. Results show increase in humidity in C-2 chamber due to water vapor release by the valve when pressure in C-1 and C-2 chambers was equal (the C-2 chamber was purged with dry nitrogen four times). At the end of the four cycles, results show valve closure after a pressure of approximately 400 Pa was applied on the membrane. The C-2 chamber was purged for a few minutes after the fourth cycle.

manometers M-1 and M-2. Two push-button valves V-1 and V-2 allow purging of the C-2 chamber with dry nitrogen. A humidity sensor (Model SHT75, size 3.7 mm × 2.2 mm × 4.9 mm, from Sensirion, Inc.) installed on the bottom of the C-2 chamber measures the relative humidity.

The valve and water reservoir assembly was installed between the C-1 and C-2 chambers, as depicted in Fig. 6. Water was supplied to the water reservoir (i.e. topside of the valve). The two chambers were kept at the same pressure. The C-2 chamber was purged with nitrogen until a humidity level of less than 1% was reached. Immediately after purging the chamber (i.e. closing the V-1 and V-2 valves), the chamber humidity started to raise indicating water vapor release by the valve. The chamber was purged with nitrogen again and the increase in the relative humidity was measured. This process was repeated several times, as the results in Fig. 7 show. Finally, pressure inside the C-2 chamber was increased approximately 400 Pa above that of the C-1 chamber by adjusting the liquid level in manometer M-2. The chamber was purged with nitrogen for several minutes. As can be seen in Fig. 7, the humidity did not rise at this point, showing that the valve was closed.

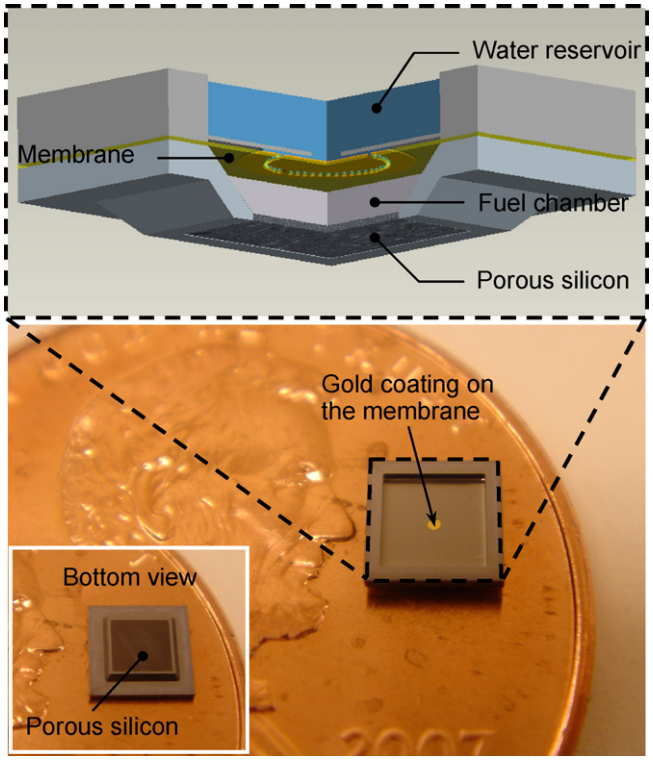

Fig. 8. Schematic assembly of the self-regulating hydrogen generator and the actual images of the top and bottom of the hydrogen generator.

4. Hydrogen generator fabrication

The hydride reactor (see its schematic cross-section in Fig. 1) was fabricated from ⟨1 0 0⟩ *p*-doped silicon using KOH etching process. The bottom wall of the hydride reactor was then anodized in 25% HF electrolyte to produce 10–20 nm diameter pores that allow hydrogen to exit the reactor. A 3D schematic of the hydride reactor assembled with the water reservoir and membrane assembly is shown in Fig. 8. A bottom image of the hydride reactor is also shown in Fig. 8, in which the porous bottom wall can be identified as the dark region in the middle of the mesa.

The hydride reactor was filled (about 60–70% of the 2.2 μL internal volume of the reactor) with $LiAlH_4$ (from Sigma–Aldrich, Inc.) in a glove box. The water reservoir and membrane assembly was then epoxied (using Scotch-Weld 2216 B/A Gray epoxy from 3M Co.) to the hydride reactor.

5. Fabrication of MEA and integration with hydrogen generator

A hybrid silicon/Nafion® MEA was fabricated on silicon-on-oxide (SOI) wafer with a 40 μm thick device layer. The handle layer of the wafer was patterned and etched in KOH solution until reached the oxide layer. The 40 μm thick device layer was then etched using DRIE process to open 100 μm × 100 μm square openings that were 100 μm apart (cf. Fig. 9) over a 1 mm × 1 mm area. Nafion® solution, ~28 μL of 5 wt.% Nafion® ionomer 1100 EW (from Solution Technology, Inc.), was then painted with a paintbrush on

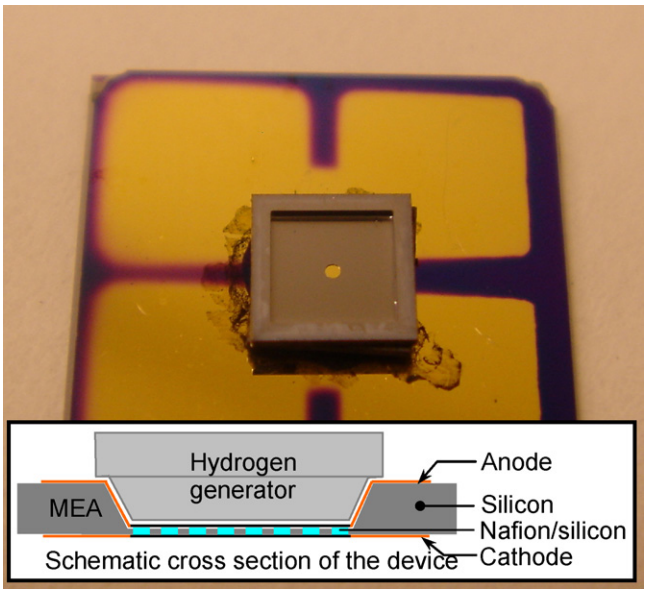

Fig. 9. Self-regulating hydrogen generator assembled on a microfabricated hybrid silicon/Nafion MEA. The image was taken before epoxy (3M Scotch-Weld 2216 B/A Gray) was poured around the micro hydrogen generator to fix it on the MEA.

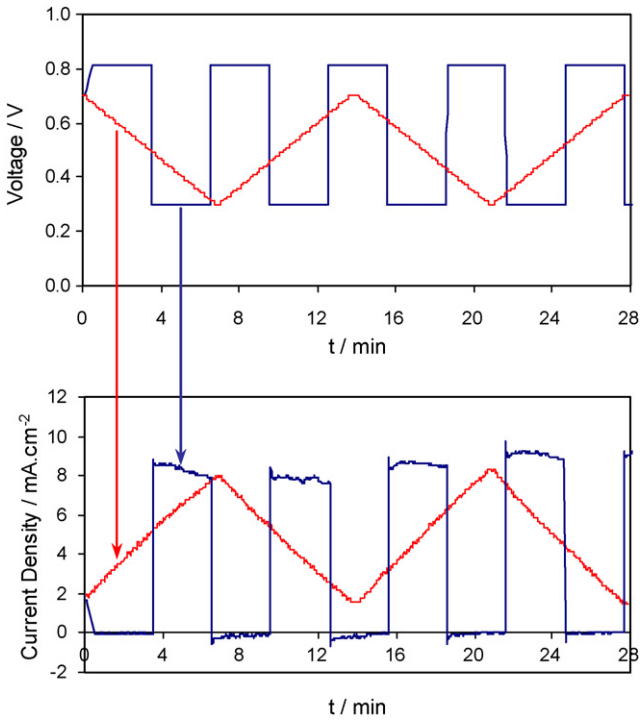

Fig. 10. Performance of the integrated device under different load conditions. Results show the device current output under varying voltage conditions. Voltage was changed in square and saw-tooth forms.

the perforated silicon membrane to fill the openings. A leak test was performed using an in-house device. Catalyst ink was then prepared by dispersing platinum black HiSPEC 1000 (from Alfa Aesar Co.) in Nafion® solution, Millipore water, and isopropanol via sonication. Using the direct paint method, the catalyst ink was painted onto the Nafion® layer of the anode and cathode. The resulting catalyst loading was approximately 20 mg cm^{-2}. In addition to the membrane area, a small amount of catalyst ink was painted onto the gold current collectors to provide electrical connection. The current collectors were made through sputter deposition of 0.1 μm thick Cr/Au layers on anode and cathode sides.

The micro hydrogen generator was then epoxied (using Scotch-Weld 2216 B/A Gray epoxy from 3 M Co.) onto the MEA to make an integrated hydrogen generator-fuel cell assembly.

6. Integrated device performance test

The integrated device was tested using a Solartron SI 1287 potentiostat. The water reservoir was filled and tests were conducted. In the first test, the voltage was switched between the open circuit voltage (~0.8 V) and 0.3 V several times (i.e. square wave form), as can be seen in Fig. 10. The primary goals of this experiment were the following.

(1) To find out if hydrogen bubbles pass through the valve and enter the water reservoir.
(2) Confirm valve closure through analysis of current transients as well as physical evidence (failure of the device due to fracture of its elements) suggesting continuous hydrogen generation and pressure build-up inside the device.

In the second test, the device voltage was changed in saw-tooth wave form between 0.3 and 0.7 V to evaluate the response of the control mechanism to gradual changes in load conditions.

7. Test results and discussions

Results of both tests are provided in Fig. 10. During the course of the experiment, no bubbles were observed to enter the water reservoir, indicating that the membrane deflection and capillary forces did not allow hydrogen to pass through the valve. Without the membrane, bubbles are observed to pass, even through long microchannels connecting the water reservoir to the hydride reactor. Also, the bottom wall of the water reservoir did not measurably bulge, suggesting that the hydrogen pressure did not increase measurably inside the device.

Analysis of the device current output also provided interesting insight about hydrogen generation. As can be seen in Fig. 10, after 3 min of device not consuming any hydrogen (i.e. open circuit mode), no spike in current (beyond the steady-state value) was observed when the voltage was dropped to 0.3 V. This test suggests that hydrogen was not produced and did not accumulate inside the device when no current was drawn. Note that higher currents can be generated with increased hydrogen pressure, considering that the MEA is capable of delivering an order of magnitude higher current (700 mA cm^{-2} at the operating voltage of 0.3 V), than what was delivered by the integrated device. The small spike (~1 mA cm^{-2} versus 8 mA cm^{-2}) seen in Fig. 10 is mainly an artifact of the experiment. A similar negative spike can be seen when current goes to zero, which suggests the spikes are due to the measurement electronics on abrupt voltage changes. Also, the near square-wave variation of the current generated showed that the hydrogen generation due to changes in the valve responded in less than a second.

The smooth variations of the output current in response to the gradual changes in voltage (i.e. saw-tooth wave form) suggested that the hydrogen generator provided sufficient hydrogen to the MEA when needed and reduced supply when the consumption rate was low.

8. Conclusions

The development of a self-regulating micro hydrogen generator for micro fuel cells was reported. The device employs a regulator micro valve for controlling the rate of hydrogen generation in a hydride reactor, eliminating the need for complex auxiliary systems commonly suggested in hydrogen generators. The control mechanism takes advantage of capillary forces to maintain water inside a confined volume connected to a water reservoir. It delivers water vapor to the hydride reactor when hydrogen pressure inside the hydride reactor is low and relies on deflection of a membrane to seal off the water reservoir from the hydride reactor when the reactor pressure increases due to excess generation of hydrogen over that consumed by the fuel cell. Several unique qualities of the hydrogen generator regulator are:

(1) It occupies a volume of less than 50 nL (approximately 0.5% of the volume of the millimeter-scale integrated device developed in this study);
(2) Unlike most other control mechanisms, it consumes no energy;
(3) It operates passively without a need for external electronics, allowing the fuel cells to operate similar to batteries; and
(4) Enables fabrication of millimeter-scale fully integrated micro fuel cells.

Acknowledgements

This research is funded by the Defense Advanced Research Projects Agency (DARPA) under grant DST 2007-0299513- 000-

1. Any opinions, findings and conclusions or recommendations expressed in this manuscript are those of the authors and do not necessarily reflect the views of the Defense Advanced Projects Research Agency or the US government.

References

[1] A. Heinzel, C. Hebling, M. Müller, M. Zedda, C. Müller, Fuel cells for low power applications, J. Power Sources 105 (2002) 250–255.
[2] M. Broussely, G. Archdale, Li-ion batteries and portable power source prospects for the next 5–10 years, J. Power Sources 136 (2004) 386–394.
[3] R. Hahn, S. Wagner, A. Schmitz, H. Reichl, Development of a planar micro fuel cell with thin film and micro patterning technologies, J. Power Sources 131 (2004) 73–78.
[4] J. Yeom, G.Z. Mozsgai, B.R. Flachsbart, E.R. Choban, A. Asthana, M.A. Shannon, P.J.A. Kenis, Microfabrication and characterization of a silicon-based millimeter scale, PEM fuel cell operating with hydrogen, methanol, or formic acid, Sens. Actuators B 107 (2005) 882–891.
[5] K.-L. Chu, S. Gold, V. Subramanian, C. Lu, M.A. Shannon, R.I. Masel, A nanoporous silicon membrane electrode assembly for on-chip micro fuel cell, J. Mems 15 (2006) 671–677.
[6] K.-L. Chu, M.A. Shannon, R.I. Masel, An improved miniature direct formic acid fuel cell based on nanoporous silicon for portable power generation, J. Electrochem. Soc. 153 (2006) 1562–1567.
[7] T. Pichonat, B. Gauthier-Manuel, Recent developments in MEMS-based miniature fuel cells, Microsyst. Technol. 13 (2007) 1671–1678.
[8] Y. Zhang, J. Lu, S. Shimano, H. Zhou, R. Maeda, Development of MEMS-based direct methanol fuel cell with high power density using nanoimprint technology, Electrochem. Commun. 9 (2007) 1365–1368.
[9] S. Tanaka, K.-S. Chang, K.-B. Min, D. Satoh, K. Yoshida, M. Esashi, Mems-based components of a miniature fuel cell/fuel reformer system, Chem. Eng. J. 101 (2004) 143–149.
[10] C. Xie, J. Bostaph, J. Pavio, Development of a 2 W direct methanol fuel cell power source, J. Power Sources 136 (2004) 55–65.
[11] S.-C. Yao, X. Tang, C.-C. Hsieh, Y. Alyousef, M. Vladimer, G.K. Fedder, C.H. Amon, Micro-electro-mechanical systems (MEMS)-based micro-scale direct methanol fuel cell development, Energy 31 (2006) 636–649.
[12] W. Qian, D.P. Wilkinson, J. Shen, H. Wang, J. Zhang, Architecture for portable direct liquid fuel cells, J. Power Sources 154 (2006) 202–213.
[13] T. Sarata, N. Yanase, T. Ozaki, T. Tamachi, K. Yuzurihara, F. Iwasaki, Method of hydrogen generation, hydrogen generator, and fuel cell apparatus, in European patent Application 06729978.4 (2006).
[14] A.V. Pattekar, M.V. Kothare, A micro reactor for hydrogen production in micro fuel cell applications, J. MEMS 13 (2004) 7–18.
[15] D.-E. Park, T. Kim, S. Kwon, C.-K. Kim, E. Yoon, Micromachined methanol steam reforming system as a hydrogen supplier for portable proton exchange membrane fuel cells, Sens. Actuators A 135 (2007) 58–66.
[16] D. Gervasio, S. Tasic, F. Zenhausern, Room temperature micro-hydrogen-generator, J. Power Sources 149 (2005) 15–21.
[17] A. Kundu, J.M. Park, J.E. Ahn, S.S. Park, Y.G. Shul, H.S. Han, Micro-channel reactor for steam reforming of methanol, Fuel 86 (2007) 1331–1336.
[18] D. Linden, Handbook of Batteries and Fuel Cells, McGraw-Hill Companies, New York, 1984.
[19] V.C.Y. Kong, D.W. Kirk, F.R. Foulkes, J.T. Hinatsu, Development of hydrogen storage for fuel cell generators. I. Hydrogen generation using hydrolysis hydrides, Int. J. Hydrogen Energy 24 (1999) 665–675.
[20] B.R. Flachsbart, K. Wong, J.M. Iannacone, E.N. Abante, R.L. Vlach, P.A. Rauchfuss, P.W. Bohn, J.V. Sweedler, M.A. Shannon, Design and fabrication of a multilayered polymer microfluidic chip with nanofluidic interconnects via adhesive contact printing, Lab-On-A-Chip 6 (2006) 667–674.